Journal of Colloid and Interface Science **248,** 67–75 (2002)
doi:10.1006/jcis.2001.8170, available online at http://www.idealibrary.com on IDEAL®

Colloid Particle Adsorption at Random Site (Heterogeneous) Surfaces

Zbigniew Adamczyk,[1] Paweł Weroński, and Elizeusz Musiał

Institute of Catalysis and Surface Chemistry, Polish Academy of Sciences, Niezapominajek 8, 30-239 Kraków, Poland

E-mail: ncadamcz@cyf-kr.edu.pl

Received August 7, 2001; accepted December 10, 2001; published online February 21, 2002

Irreversible adsorption of colloid particles and globular proteins at heterogeneous surfaces was studied theoretically. The substrate surface was created by covering a uniform surface by coupling sites (active centers) of a desired coverage. In contrast to previous studies concerned with disks, in our simulations the centers were modeled by spheres having a size smaller than that of the adsorbing particles. Adsorption was assumed to occur due to short-ranged attractive interactions if the colloid particle contacted the center. The Monte-Carlo-type simulations enabled one to determine the initial flux, adsorption kinetics, jamming coverage, and the structure of the particle monolayer as a function of the site coverage and the particle/site size ratio, denoted by λ. It was revealed that the initial flux increased significantly with the site coverage θ_s and the λ parameter. This behavior was quantitatively interpreted in terms of the scaled particle theory. It also was demonstrated that particle adsorption kinetics and the jamming coverage increased significantly, at fixed site coverage, when the λ parameter increased. Practically, for $\alpha = \lambda^2\theta_s > 1$ the jamming coverage at the heterogeneous surfaces attained the value pertinent to continuous surfaces. The results obtained prove unequivocally that the spherically shaped sites are much more effective in binding particles than the disk-shaped sites considered previously. © 2002 Elsevier Science (USA)

Key Words: **adsorption of colloids; colloid adsorption; heterogeneous surface adsorption; irreversible adsorption; kinetics of particle adsorption; protein adsorption; random site adsorption.**

INTRODUCTION

Adsorption and deposition (irreversible adsorption) of colloids, proteins, and other biomaterials on solid/liquid interfaces are of large significance for many practical and natural processes such as filtration, paper making, thrombosis, separation of biomaterial-like proteins, bacteria, viruses, enzymes, and pathological cells. Kinetics of these processes is regulated by the use of coupling agents bound to interfaces which promote adherence of particles. For example, cationic polyelectrolytes are used to increase retention of filler particles in paper-making processes (1, 2) or to promote a selective self-assembly of colloid particles at patterned surfaces (3). In biological applications special proteins (ligands) attached to the surface are applied for a selective binding of a desired solute from protein mixtures as is the case in the affinity chromatography (4). Analogously, in immunological assays (5, 6) one is often using special proteins (antibodies) attached electrostatically or covalently to colloid particles (e.g., polystyrene latex) to promote selective adsorption of other proteins (antigens) present in the serum. This leads to aggregation (agglutination) of the colloid suspension, which can easily be evidenced experimentally (7).

Similarly, many studies on colloid particle adsorption involved surfaces modified by polymers (8, 9), surfactants (10), or chemical coupling agents (silanes) used to change the natural surface charge of substrate surfaces (11). This is often the case with natural mica used as molecularly smooth substrate in many particle deposition studies (12).

A characteristic feature of the above-mentioned processes is that particle or protein adsorption occurs at surfaces that are inherently heterogeneous. This raises an important question on how the size, shape, and surface concentration of adsorption sites (which can be treated in the classical adsorption terminology as active centers) influences the kinetics of particle adsorption. One is also interested in predicting *a priori* the maximum (jamming) coverage of particles attainable for a given concentration of sites.

Despite the significance of these processes few works in the literature with the exception of the papers of Jin *et al*. (13, 14), who studied theoretically irreversible adsorption of particles at nonuniform surfaces covered by point-like adsorption sites, have been reported. These surfaces were referred to as random site surfaces (RSS). A correspondence (mapping function) between the adsorption process at nonuniform surfaces and the widely studied random sequential adsorption (RSA) over continuous surfaces (11, 15–17) was found.

These results have been generalized to the experimentally more interesting situation when adsorption sites have finite dimensions, comparable with the adsorbing particle size (18). Adsorption kinetics and jamming coverage was determined via Monte-Carlo-type simulations as a function of the particle/site size ratio and their coverage. However, the validity of these results is limited by the fact that the sites were modeled as flat disks incorporated into the substrate. Such a site configuration is rather specific and difficult to realize in practice.

[1] To whom correspondence should be addressed.

0021-9797/02 $35.00
© 2002 Elsevier Science (USA)
All rights reserved.

Therefore, the goal of this paper is to derive similar results for the experimentally more interesting situation of active sites formed by smaller-sized spherical particles attached irreversibly to a homogeneous interface.

THE THEORETICAL MODEL

We consider the following model of irreversible adsorption of colloid particles over heterogeneous surfaces. The sites (surface heterogeneities) were represented by hard spheres of radius a_s (see Fig. 1). There were N_s^o spheres distributed over a homogeneous surface having the geometrical surface area ΔS. Without loss of generality one can assume $\Delta S = 1$ and normalize accordingly the sphere dimension. The surface concentration (2D density) of the sites is then equal to N_s^o, and the dimensionless coverage is defined as $\theta_s = \pi a_s^2 N_s^o$. The configuration of the sites can be produced in a number of ways, e.g., by quenching an equilibrium fluid of a given coverage, or by performing RSA simulations (11, 19), which was the procedure adopted in our work.

The basic assumption of our model is that the colloid particle (of a spherical shape) can only be adsorbed upon touching the site, see Fig. 1. Otherwise, at bare interface, the particle will not adsorb. Physically, this corresponds to the situation when the particles are irreversibly bound to the sites due to short-ranged attractive interactions of an electrostatic or chemical nature.

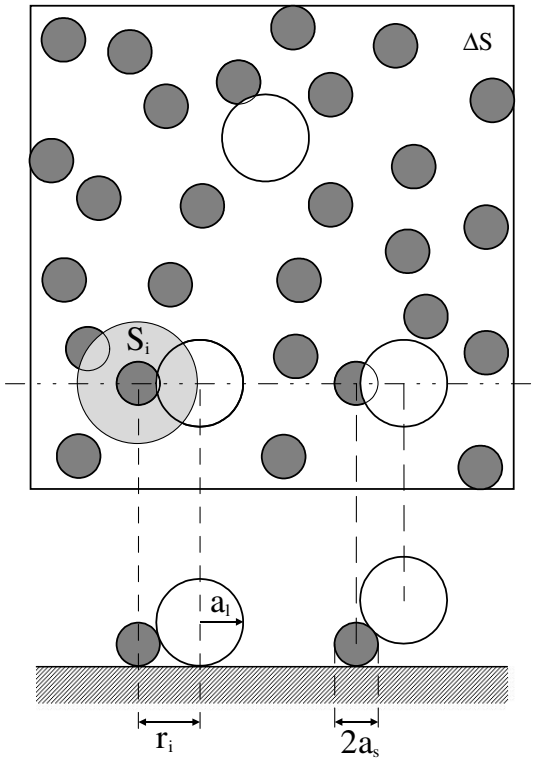

FIG. 1. A schematic representation of particle adsorption over heterogeneous surfaces bearing spherically shaped adsorption sites.

Furthermore, particle adsorption was assumed irreversible and localized, which means that particle position at the site remained fixed during the entire simulation run.

In accordance with these assumptions, particle adsorption at the heterogeneous surfaces was modeled according to the following algorithm:

(i) An adsorbing (virtual) particle of radius a_l was generated at random within the simulation area; if it did not touch any of the heterogeneities the particle was rejected and another virtual particle was produced (the number of attempts N_{att} was increased by 1).

(ii) Otherwise, if the particle touched any of the sites, the overlapping test was performed according to the usual RSA rules; i.e., it was checked whether there is any previously adsorbed particle within the exclusion volume (see Fig. 1). If there was overlapping, the simulation loop was repeated (the number of attempts was increased by 1).

(iii) If there was no overlapping, the virtual particle was assumed irreversibly adsorbed at the given position and its coordinates were stored, the number of adsorbed particles N_p being increased by 1.

It should be mentioned that particle adsorption at heterogeneous surfaces modeled by spherically shaped sites is a truly three-dimensional process, opposite to adsorption at disk-shaped sites considered previously (18). Hence, the adsorbed particle centers are located in various planes which influenced both adsorption kinetics and the coverage of particles.

As usual in the RSA simulation the coverage was calculated as $\theta_l = \pi a_l^2 N_p$. On the other hand, the dimensionless computer adsorption time is defined as (11, 13, 14, 18, 19)

$$\tau = \pi a_l^2 \frac{N_{att}}{\Delta S} = \pi a_l^2 N_{att}. \qquad [1]$$

By plotting θ_l vs the adsorption time τ defined above, one can simulate the kinetics of particle adsorption.

An alternative evaluation of particle adsorption kinetics can be achieved via the available surface function (ASF) approach (13, 14, 18, 19). This function can be defined as normalized probability p of adsorbing a particle for a given configuration of sites, their coverage θ_s, and the particle coverage θ_l. Additionally, the ASF is dependent on the particle to site size ratio a_l/a_s denoted by λ. This function can effectively be evaluated from simulations by performing, at fixed θ_s and θ_l, a large number of adsorption trials N_{att}, N_{succ} of them being potentially successful. Then the ASF is defined as the limit of N_{succ}/N_{att} when $N_{att} \to \infty$. In practice, due to computer time limitations, N_{att} was about 10^5. Especially important is the value of ASF in the limit of negligible particle coverage, $\theta_l = 0$ since it characterizes the initial flux to heterogeneous surfaces. This quantity is of a primary interest from an experimental viewpoint. Knowing ASF one can calculate particle adsorption kinetics by integrating the

constitutive dependence (13–17)

$$\frac{d\theta_l}{d\tau} = p. \qquad [2]$$

As discussed in (20) this classical concept of the ASF may be not general enough to deal with the diffusion-controlled adsorption of particles. More refined approaches, considering various transport mechanisms of particles in the bulk, have been proposed (21–23). However, due to insurmountable mathematical problems, their applicability for heterogeneous surface adsorption seems prohibitive. Therefore, in this work, we adopt the standard ASF concept which reflects the most important features of the problem of particle adsorption at heterogeneous surfaces. This function can be used for specifying boundary conditions for the bulk transport equation as shown in (24).

The pair correlation function $g(r_l)$ (often referred to θ_s as the radial distribution function RDF) was calculated by generating particle populations according to the above RSA scheme and exploiting the definition (19)

$$g(r) = \frac{\pi a_l^2}{\theta_l}\left\langle \frac{\Delta N_p}{2\pi r \Delta r}\right\rangle, \qquad [3]$$

where $\langle\ \rangle$ means the ensemble average and ΔN_p is the number of particles adsorbed within the ring $2r\Delta r$ drawn around a central particle. It should be mentioned that the distance r was measured between the projection of the adsorbed particle centers on the adsorption plane. Obviously, all particles located close to the perimeter of the simulation area were discarded from the averaging procedure. In order to obtain a satisfactory accuracy of $g(r)$, particle populations reaching 10^5 were considered.

RESULTS AND DISCUSSION

Limiting Analytical Expressions

Despite simple rules, the topology and kinetics of particle adsorption at heterogeneous surfaces is rather complex, especially at a higher coverage θ_l. Due to the high dimensionality of this problem, no analytical results of a general validity can be formulated. However, useful limiting expressions can be derived for the low coverage of adsorbed particles. These expressions having a practical significance can be exploited for testing the validity of numerical simulations.

From simple geometrical considerations one can deduce that the particle adsorbs if the distance between its center projected on the adsorption plane and the site center r_i becomes smaller than $2\sqrt{a_l a_s}$ (see Fig. 1). Hence the interaction area of the particle with the site is

$$S_i = \pi r_i^2 = 4\pi a_l a_s. \qquad [4]$$

If the site distribution can be treated as uniform, the probability of finding any site within the interaction area can be calculated from the Poisson distribution as

$$p_0 = 1 - e^{-S_i N_s^0} = 1 - e^{-4\lambda\theta_s}. \qquad [5]$$

One can deduce from Eq. [5] that in the limit of $\theta_s < 1/4\lambda$, $p_0 = 4\lambda\theta_s$.

This probability, which can be identified with the ASF, describes the initial flux of particles when $\theta_l = 0$.

Obviously, Eq. [5] becomes less accurate in the limit of larger θ_s when the distribution of the sites deviates from a uniform distribution (11, 19). A more accurate expression can be formulated by exploiting the results discussed in (19). By exploiting the scaled particle theory of Reiss *et al*. (25) it was demonstrated that the probability of finding a cavity of surface area S_i devoid of sites (smaller sized particles) is given by the formula

$$p_c = B_l^0 = (1-\theta_s)e^{-\frac{(4\lambda-1)\theta_s}{1-\theta_s} - \left[\frac{(2\sqrt{\lambda}-1)\theta_s}{1-\theta_s}\right]^2}, \qquad [6]$$

where B_l^0 is defined as the surface blocking function for the analogous problem of particle adsorption over surfaces precovered with smaller sized particles (when adsorption occurs at the uncovered interface only). Since the probability of finding a site within the interaction area equals $1 - p_c$ one can predict that

$$p_0 = 1 - B_l^0 = 1 - (1-\theta_s)e^{-\frac{(4\lambda-1)\theta_s}{1-\theta_s} - \left[\frac{(2\sqrt{\lambda}-1)\theta_s}{1-\theta_s}\right]^2}. \qquad [7]$$

Formulas [5] and [7] are valid for initial stages of adsorption when $\theta_l = 0$. In the case when θ_l is finite but the site coverage remains small, so $\theta_s < 1/4\lambda$, the adsorption probability of particles can be expressed via the Langmuir-like formula

$$p = S_i\left(N_s^0 - N_p/n_s\right)(1 - q\theta_l), \qquad [8a]$$

where n_s is the site multiplicity to be determined from numerical simulations and the multiplier $1 - q\theta_l$ accounts for exclusion effects among particles (lowest order correction). From simple geometry one can deduce that for $\lambda > 4$ one site can coordinate only one particle, so $n_s = 1$.

Equation [7] can be rearranged to

$$\begin{aligned} p &= 4\lambda\theta_s(1 - \theta_l/\lambda^2\theta_s n_s)(1 - q\theta_l) \\ &\cong p_0\left(1 - \theta_l/\theta_l^{mx}\right), \end{aligned} \qquad [8b]$$

where

$$\theta_l^{mx} = \frac{\lambda^2 n_s \theta_s}{1 + q\lambda^2 n_s \theta_s} \qquad [9]$$

can be treated as the maximum coverage of large particles in the limit when the site coverage becomes low.

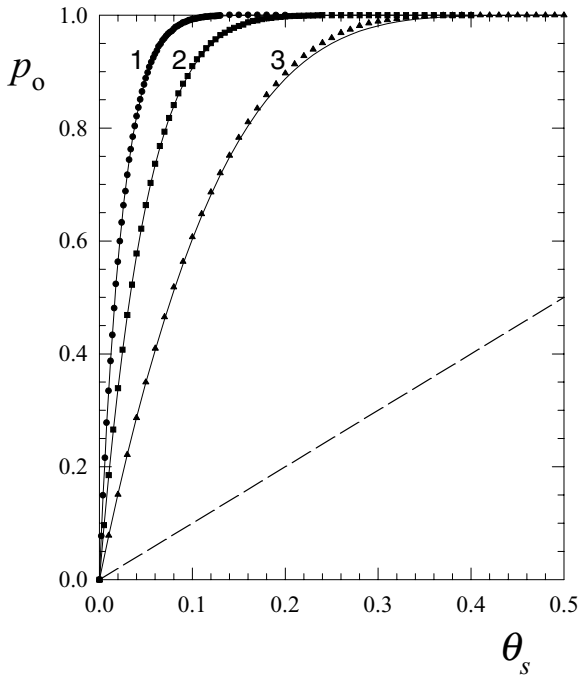

FIG. 2. The dependence of the initial adsorption probability p_0 on surface coverage of adsorption sites θ_s; the points denote numerical simulations performed for (1) ●, $\lambda = 10$; (2) ■, $\lambda = 5$; and (3) ▲, $\lambda = 2$. The solid lines represent the analytical results derived from Eq. [7], and the broken line shows the analytical predictions for adsorption on disks, when $p_0 = \theta_s$ (18).

Numerical Results

The numerical calculations discussed hereafter concerning the ASF, adsorption kinetics, jamming coverage, and pair correlation function have been carried out for the values of $\lambda = 2$, 5, and 10, which seem typical for practically occurring situations.

As mentioned, the quantity of a primary practical interest is the p_0 function, which represents the averaged probability of adsorbing the particle at surfaces covered by a given number of sites. Hence, by knowing p_0 one can calculate the initial flux of solute (particles) to heterogeneous surfaces. The dependence of p_0 on θ_s calculated for $\lambda = 2$, 5, and 10 is plotted in Fig. 2. As can be noticed, the adsorption probability of particles increases abruptly with θ_s, especially for larger λ values. For $\lambda = 10$, the probability of adsorption reaches unity (the value pertinent to homogeneous surfaces) for θ_s as low as 10%. This behavior is well reflected by Eq. [7] being in a quantitative agreement with the numerical data for the entire range of θ_s and λ studied. It is also interesting to note that adsorption probability at spherical sites becomes considerably larger than that for circular sites, when $p_0 = \theta_s$ (18), depicted by the broken line in Fig. 2. This observation has practical implications, showing that the geometry of the active sites plays a more decisive role than their surface concentration. The results shown in Fig. 2 further imply that by measuring experimentally the flux of larger colloid particles (which can easily be done by direct microscope observations) one can detect the presence of nanoscale surface heterogeneities, invisible under the microscope. If the surface concentration of the sites can be estimated, one can determine their size or shape from the particle deposition experiments.

The validity of the theoretical results shown in Fig. 2 has been confirmed in experiments involving polystyrene latex particles adsorbing at sites produced from smaller sized particles preadsorbed at mica (26).

One should remember, however, that the results shown in Fig. 2 describe the particle adsorption rate at heterogeneous surfaces in the limit when their accumulation is negligible, i.e., for $\theta_l \to 0$ only. If θ_l becomes finite, the probability of particle adsorption decreases as a result of volume exclusion effects (often referred to less accurately as surface blocking effects). The adsorption probability (ASF) is then a function of θ_s, θ_l, and λ. It was found in the simulations that a more universal behavior exhibits the reduced ASF function p/p_0, which is plotted in Fig. 3 for $\lambda = 2$ and in Figs. 4 and 5 for $\lambda = 5$ and 10, respectively. As can be observed in Fig. 3, for $\theta_l < 0.1$ the p/p_0 function can be well reflected by the Langmuir-like model, described by Eq. [8]. The site multiplicity parameter n was found from numerical simulations to be 2.45 (in the limit of low coverage θ_l), whereas the q parameter was assumed equal to 4, which corresponds to the exclusion area of two spherical particles (10, 16). On the other hand, for $\theta_l > 2$ the p/p_0 function becomes independent of θ_s and approaches the universal curve derived from the classical RSA model (16, 17) for homogeneous

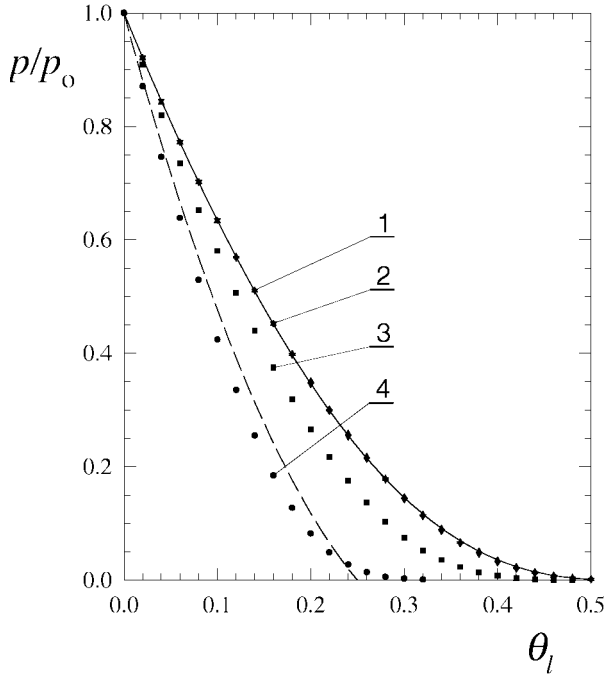

FIG. 3. The dependence of the reduced ASF, p/p_0 on θ_l; the points denote numerical results obtained for $\lambda = 2$ and (1) ▼, $\theta_s = 0.5$ ($\alpha = 2$); (2) ▲, $\theta_s = 0.2$ ($\alpha = 0.8$); (3) ■, $\theta_s = 0.1$ ($\alpha = 0.4$); and (4) ●, $\theta_s = 0.05$ ($\alpha = 0.2$). The solid lines represent the results for the RSA model of homogeneous surfaces, Eq. [11], and the dashed line shows the results calculated from Eq. [8b].

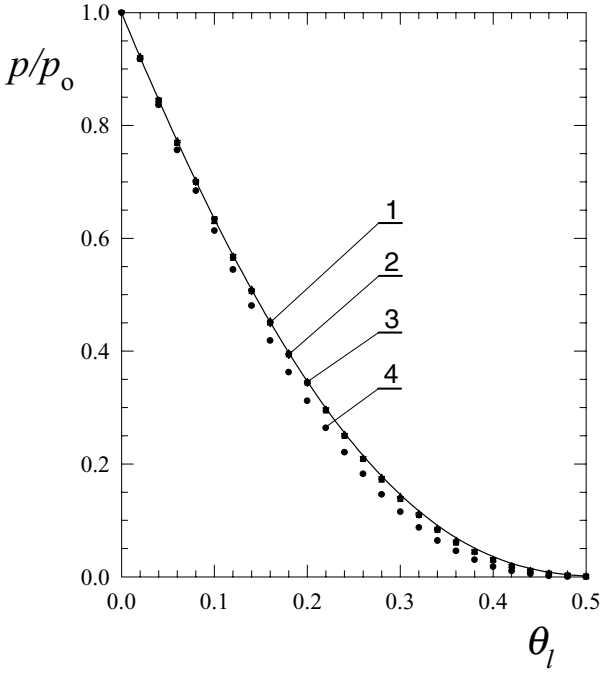

FIG. 4. The dependence of the reduced ASF, p/p_0 on θ_l; the points denote numerical results obtained for $\lambda = 5$ and (1) ▼, $\theta_s = 0.5$ ($\alpha = 12.5$); (2) ▲, $\theta_s = 0.2$ ($\alpha = 5.0$); (3) ■, $\theta_s = 0.1$ ($\alpha = 2.5$); and (4) ●, $\theta_s = 0.05$ ($\alpha = 1.25$). The solid line represent the results obtained for the RSA model of homogeneous surfaces, Eq. [11].

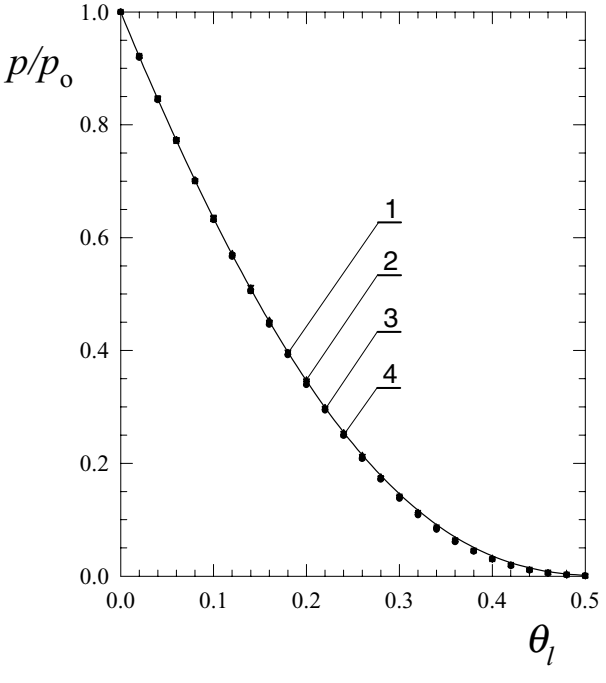

FIG. 5. The dependence of the reduced ASF, p/p_0 on θ_l; the points denote numerical results obtained for $\lambda = 10$ and (1) ▼, $\theta_s = 0.5$ ($\alpha = 50$); (2) ▲, $\theta_s = 0.2$ ($\alpha = 20$); (3) ■, $\theta_s = 0.1$ ($\alpha = 10$); and (4) ●, $\theta_s = 0.05$ ($\alpha = 5.0$). The solid line represents the results obtained for the RSA model of homogeneous surfaces, Eq. [11].

surface adsorption. Similar results were observed for $\lambda = 5$ and 10, as can be seen in Figs. 4 and 5. One can, therefore, summarize these results by expressing the postulate that in the case when $\alpha = \lambda^2\theta_s > 1$ particle adsorption at heterogeneous surfaces is governed by the function

$$p = p_0 B(\theta_l), \qquad [10]$$

where the function $p_0(\lambda, \theta)$ is given by Eq. [7] and $B(\theta_l)$ can be calculated from various analytical fitting functions of the type (16, 17)

$$B(\bar{\theta}_l) = f(\bar{\theta}_l)(1 - \bar{\theta}_l)^3, \qquad [11]$$

where $\bar{\theta} = \theta_l/\theta_l^\infty$, θ_l^∞ is the jamming coverage, and $f(\bar{\theta}_l)$ are low-order polynomials. One of the most accurate expressions for $f(\bar{\theta}_l)$ has the form (16)

$$f(\bar{\theta}_l) = 1 + 0.812\bar{\theta}_l + 0.426\bar{\theta}_l^2 + 0.0716\bar{\theta}_l^3. \qquad [12]$$

As can be deduced from Eqs. [11 and 12], in the limit when $\bar{\theta}_l \to 1$ the blocking function assumes the form

$$B(\bar{\theta}) \cong 2.31(1 - \bar{\theta}_l)^3. \qquad [13]$$

It is interesting to note that Eq. [13] can be derived by topological arguments as discussed in (15–17). Thus, according to Eq. [10] the $(p/p_0)^{1/3}$ function for the heterogeneous surfaces should depend linearly on θ_l. The numerical results plotted using this transformation in Fig. 6 confirm this hypothesis. This has significant practical implications because all the results known previously for homogeneous surfaces can directly be transferred to heterogeneous surface adsorption. In particular, by substituting the expression for the ASF given by Eq. [10] into the constitutive dependence, Eq. [2], one obtains

$$\int^{\theta_l} \frac{d\bar{\theta}'}{B(\bar{\theta}')} = p_0\tau/\theta_l^\infty = \tau'. \qquad [14]$$

One can deduce from Eq. [14] that all the kinetic results known previously for the continuous surfaces can be directly transferred to heterogeneous surfaces by introducing the transformed adsorption time $\tau' = p_0(\theta_s, \lambda)/\theta_l^\infty\tau$. In particular, by substituting Eq. [13] into Eq. [14] one obtains upon integration the limiting result

$$\theta_l(\tau') = \theta_l^\infty\left(1 - \frac{C}{\sqrt{\tau'}}\right), \qquad [15]$$

where

$$C = \sqrt{\frac{\theta_l^\infty}{4.62p_0}}.$$

However, in the general case, with $B(\bar{\theta}_l)$ given by Eq. [11], the integration procedure is rather awkward. Jin *et al.* (13, 14)

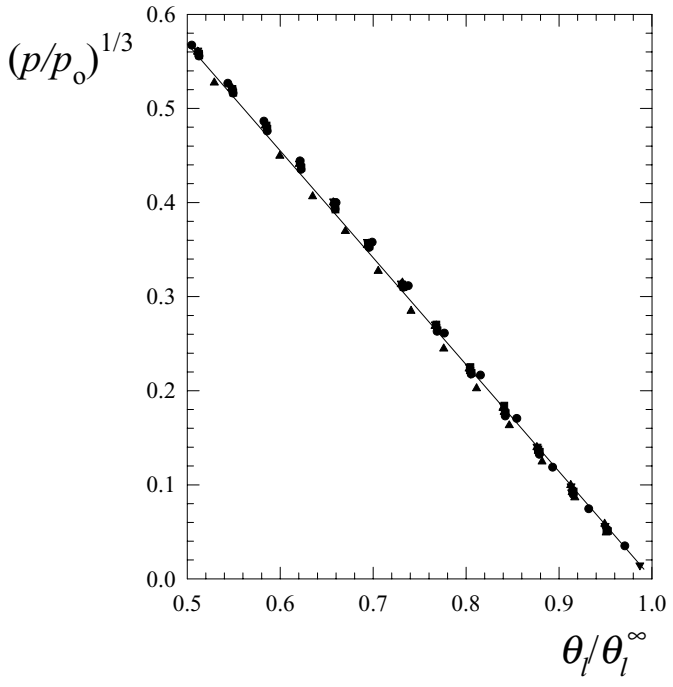

FIG. 6. The dependence of $(p/p_0)^{1/3}$ on the reduced coverage $\bar{\theta}_l = \theta_l/\theta_l^\infty$; the points denote numerical simulations, performed for various λ and θ_s. The solid line represents the analytical approximation calculated from Eq. [15].

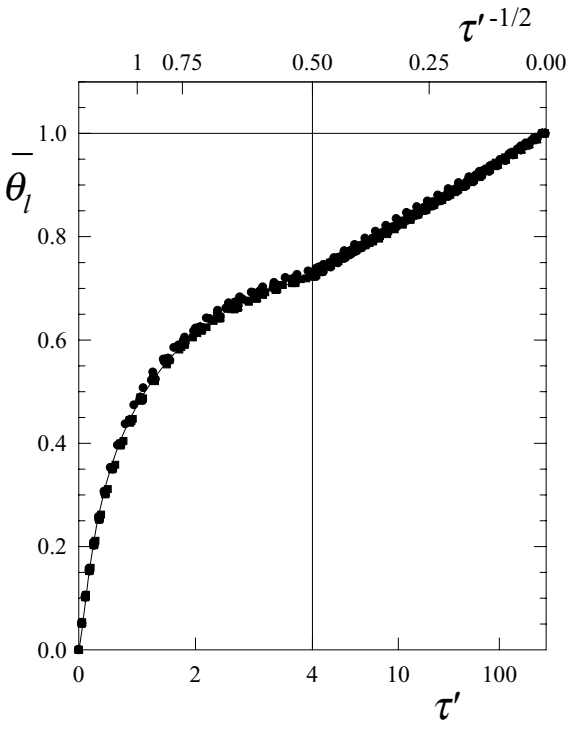

FIG. 7. Particle adsorption kinetics expressed in the universal coordinate system θ_l/θ_l^∞ vs $\tau' = \tau p_0/\theta_l^\infty$; the points denote the numerical simulations performed for various θ_s and λ, and the solid line represents the limiting results for continuous surfaces (RSA model), calculated from Eq. [16].

derived the following interpolation function which adequately interpolates the data for the entire range of times

$$\theta_l = \theta_\infty\left(1 - \frac{1 + 0.314\tau'^2 + 0.45\tau'^3}{1 + 1.83\tau' + 0.66\tau'^3 + \tau'^{7/2}}\right), \qquad [16]$$

where τ' is the transformed adsorption time.

The numerical data expressed using the above transformation for various λ and θ_s are plotted in Fig. 7. As one can notice for $\alpha > 1$ the simulations approach the universal kinetic curve given by Eq. [16], which validates the hypothesis expressed via Eq. [10]. The jamming coverage θ_l^∞ needed for the time transformation was obtained as previously done for continuous surfaces (19) by a linear extrapolation of numerical results to infinite time (in the coordinate system θ_l vs $(\tau')^{-1/2}$).

Because the jamming coverage θ_l^∞ has a fundamental practical significance we performed extensive simulations aimed at determining this parameter as a function of θ_s and λ. The results plotted as θ_l^∞ vs θ_s (in logarithmic scale) are collected in Fig. 8. The analytical results predicted from the low coverage dependence, i.e., $\theta_l = \lambda^2\theta_s$, are also plotted for comparison (dashed lines in Fig. 8). As can be noticed this analytical formula works for $\lambda^2\theta < 0.02$ only. It was found that for higher site coverage the numerical results can be well interpolated by the simple analytical function

$$\theta_l^\infty = \theta_\infty\left(1 - e^{-\frac{\lambda^2\theta_s}{\theta_\infty}}\right). \qquad [17]$$

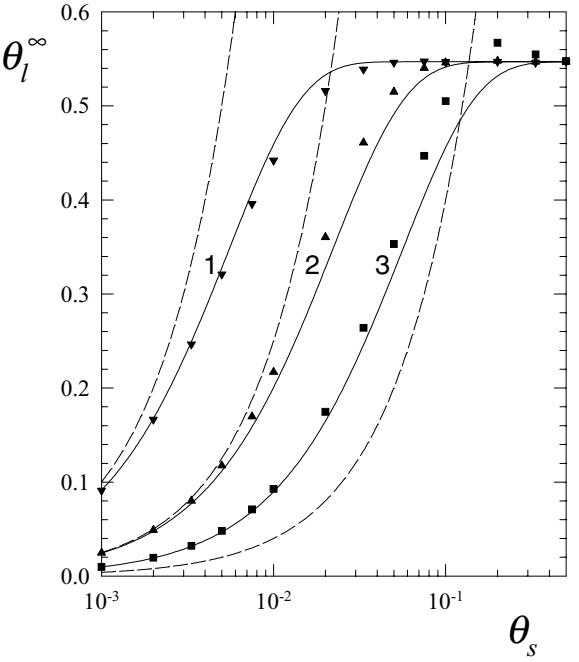

FIG. 8. The dependence of the jamming coverage of particles θ_l^∞ on the coverage of the adsorption sites θ_s; the points denote the results of numerical simulations, performed for (1) ▼, $\lambda = 10$; (2) ▲, $\lambda = 5$; (3) ■, $\lambda = 2$. The solid lines represent the fitting functions given by Eq. [18], and the dashed lines show the results derived from the Langmuir model, i.e., $\theta_l = \lambda^2\theta_s$.

This formula gives a satisfactory accuracy for the entire rang of θ_s studied. However, it breaks down for $\lambda = 2$ probably due to the site multiplicity effect discussed previously. Moreover, in this case, a maximum on the θ_l vs θ_s dependence is observed for θ about 0.25. This maximum jamming coverage attains the value of 0.57, being slightly larger than that for adsorption at uniform surfaces. The maximum appears because, for θ_s about 0.2–0.3, the area accessible for particle adsorption becomes larger than the geometrical interface area, which can be interpreted as apparent roughness effect. When θ_s increases further above this critical value, the accessible area becomes again very close to the geometrical interface area. Although this effect is interesting from a theoretical point of view, it will be difficult to measure experimentally. This is so because in practice it is very difficult to measure the surface coverage of particles with a relative accuracy better than 5% due, for example, to the polydispersity effects (27).

It was found that a reasonable fitting function for the case $\lambda = 2$ has the form

$$\theta_l^{\infty} = \theta_{\infty}\left(1 - e^{-\frac{n_s\lambda^2\theta_s}{\theta_{\infty}}}\right). \qquad [18]$$

Except for the region near the maximum, and $\theta_s < 0.002$, this function ensures a uniform fit of the numerical data with an accuracy better than a few percent. It is worthwhile noting that the jamming coverage in the case of spherical adsorption sites increases with θ_s in a more efficient way (for $\theta_s > 0.05$) than that for disk-shaped sites (18). In the latter case the jamming coverage for $\lambda > 2$ was well reflected by the rational function.

Once θ_l^{∞} is known one can unequivocally evaluate the blocking function $B(\theta_l)$ via Eq. [11] and particle adsorption kinetics via Eq. [14] or its integrated form, Eq. [16]. As discussed in some detail elsewhere (22, 24, 28) such an approach is only valid when the thickness of the diffusion boundary layer remains comparable with the adsorbing particle dimension. This requirement is fulfilled for micrometer-sized particles under forced convection transport conditions only (28). For smaller particles and the diffusion-controlled transport conditions the coupling between the bulk and surface transport should be considered via the approach developed in (24, 27, 28) for uniform surfaces. According to this model, Eq. [10] can be exploited as the boundary condition for the bulk transport problems. In this way the main features of particle adsorption at a heterogeneous surface can be properly reflected, in particular the initial adsorption rate and the jamming coverage. However, due to complicated topology, a more detailed description of these processes requires further theoretical studies.

Besides kinetic aspects, in many applications of practical interest, e.g., colloid lithography, one is interested in the structure of the particle monolayer. The structure is directly characterized in terms of the pair correlation function $g(r)$. It was determined from particle populations generated in simulations according to the procedure described above. As mentioned, in order to attain a satisfactory accuracy of the pair correlation function $g(r)$, particle populations reaching 10^5 were considered by averaging over many simulation runs. The distributions of g derived from numerical simulations for $\theta_s = 0.1$, $\lambda = 2$, and various θ_l are shown in Fig. 9. Similar results obtained for $\lambda = 2$, $\theta_l = 0.5$, and site coverage θ_s ranging from 0.1 to 0.5 are

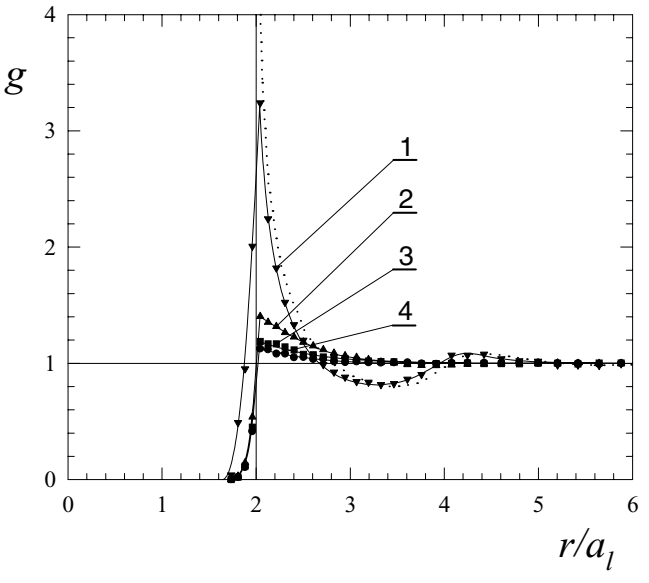

FIG. 9. The pair correlation function of particles g derived from numerical simulations for the heterogeneous surfaces, $\lambda = 2$, $\theta_s = 0.1$: (1) ▼, $\theta_l = 0.5$; (2) ▲, $\theta_l = 0.2$; (3) ■, $\theta_l = 0.1$; (4) ●, $\theta_l = 0.05$. The dotted lines denote the results pertinent to uniform surfaces (derived from the standard RSA model).

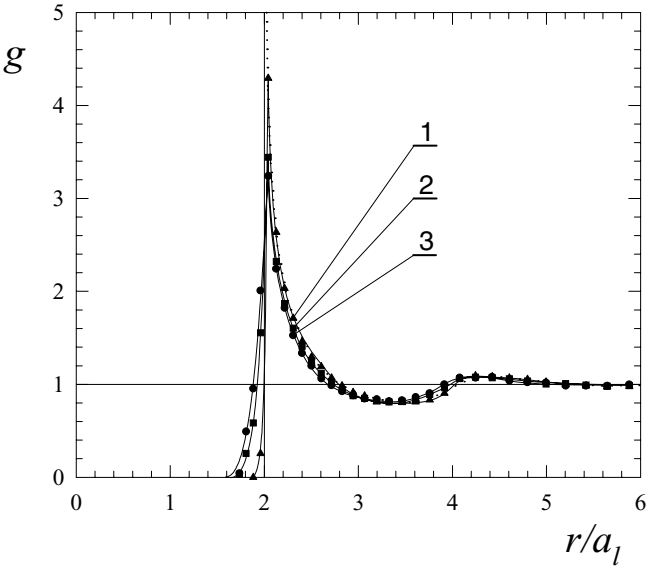

FIG. 10. The pair correlation function g derived from numerical simulations for the heterogeneous surfaces, $\lambda = 2$, $\theta_l = 0.5$: (1) ▲, $\theta_s = 0.5$; (2) ■, $\theta_s = 0.2$; (3) ●, $\theta_s = 0.1$. The dotted lines represent the pair correlation function pertinent to uniform surfaces (derived from the standard RSA model).

plotted in Fig. 10. As can be observed the structure of particle monolayers for $\lambda = 2$ at heterogeneous surfaces resembles closely the structure monolayer predicted theoretically and observed at homogeneous surfaces for polydisperse particle systems (27). This indicates that adsorption at sites occurs in various planes, so particle projections on the interface can overlap. This is reflected by the $g(r)$ function which remains finite for $r < 2$. It should be mentioned, however, that the apparent overlapping effect becomes negligible for site coverage exceeding 0.2 (cf. Fig. 10). In this case the structure of particle monolayers becomes practically identical with the structure generated in the RSA processes at homogeneous surfaces. Similarly, as can be seen in Fig. 11, for increased λ (larger particle to site size ratio) the structure of particle monolayers at heterogeneous surfaces becomes practically indistinguishable from that at homogeneous surfaces.

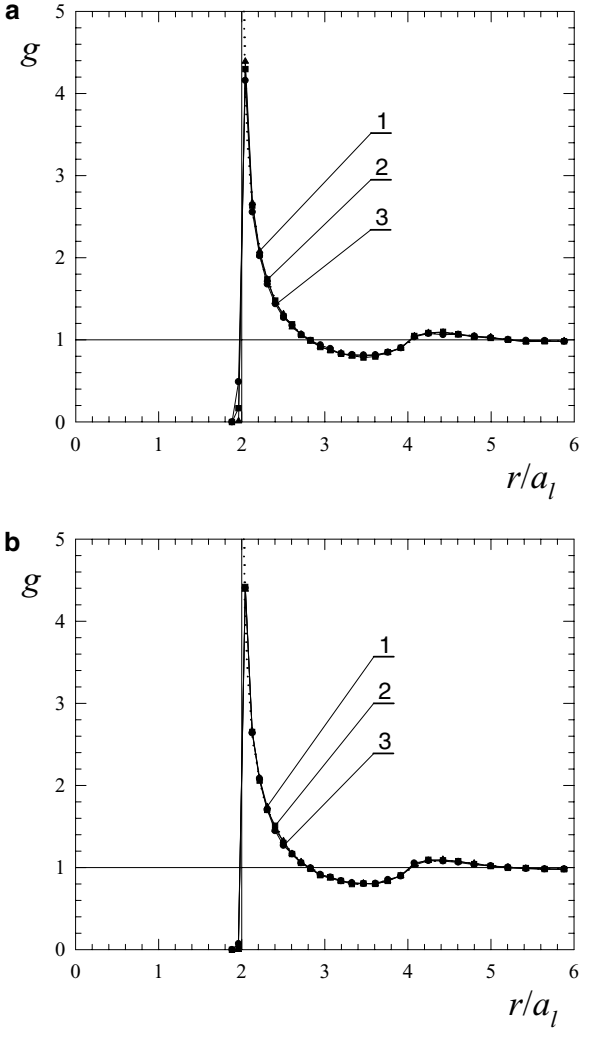

FIG. 11. The pair correlation function g derived from numerical simulations for $\theta_l = 0.5$, (1) ▲, $\theta_s = 0.5$; (2) ■, $\theta_s = 0.2$; (3) ●, $\theta_s = 0.1$. The dotted lines represent the pair correlation function pertinent to uniform surfaces (derived from the standard RSA model). (a) $\lambda = 5$, and (b) $\lambda = 10$.

It should be mentioned that all the results obtained in this work concern hard particle adsorption problems, when the range of interactions is much smaller than particle dimension. Such a situation can be realized experimentally for high electrolyte concentration when the electrostatic double-layer interactions are eliminated (12). For dilute electrolytes the interaction becomes comparable with particle size, which affects both adsorption kinetics and the jamming coverage. The latter parameter for interacting systems can be calculated using the effective hard particle concept developed in (11). However, the range of the validity of this approximation can only be estimated by comparison with numerical simulations planned in the future.

CONCLUDING REMARKS

It was demonstrated that the initial adsorption rate of particles at surfaces covered by spherical adsorption sites is well reflected by Eq. [7], which indicates that for $\theta_s > 1/4\lambda$, the rate attains the maximum value characteristic of homogeneous surfaces. In this respect the adsorption of particles at spherical sites is much more efficient than adsorption at disks studied previously. The validity of the simulations and Eq. [7] has been confirmed in model experiments involving polystyrene latex particles adsorbing at oppositely charged sites attached to mica (26).

On the other hand, for $\theta_s < 1/4\lambda$ and $\theta_l > 0$ the particle adsorption rate is given by the quasi–Langmuir model

$$p = p_0\left(1 - \theta/\theta_l^{mx}\right) = 4\lambda\theta_s\left(1 - \theta/\theta_l^{mx}\right),$$

where the apparent saturation coverage θ_l^{mx} is given by Eq. [9].

If the inequality $\alpha = \lambda^2\theta_s > 1$ is fulfilled (high site density limit) the particle adsorption rate is described by the formula

$$p = p_0 B(\theta_l),$$

where $B(\theta_l)$ is the blocking function derived from the standard RSA model for homogeneous surfaces, given explicitly by Eqs. [11 and 12]. This indicates that all the results known previously for homogeneous surfaces can be directly transferred to heterogeneous surfaces by an appropriate adsorption time transformation. In particular one can deduce that adsorption kinetics is given by Eq. [16] with the reduced adsorption time $\tau' = p_0\tau/\theta_l^{\infty}$. The jamming coverage θ_l^{∞} needed in this transformation can be calculated from the simple interpolating function

$$\theta_l^{\infty} = \theta_{\infty}\left(1 - e^{-\frac{n_s\lambda^2\theta_s}{\theta_{\infty}}}\right),$$

where the site multiplicity parameter n_s was found equal to 2.45 for $\lambda = 2$ and equal to 1 for $\lambda > 4$.

From the numerical simulations it was also deduced that the structure of particle monolayers formed at heterogeneous surfaces resembles closely that at homogeneous surfaces if $\lambda > 2$.

ACKNOWLEDGMENT

This work was supported by the KBN Grant 3T09A 105 18.

REFERENCES

1. Boluk, M. Y., and van de Ven, T. G. M., *Colloids Surf.* **46,** 157 (1990).
2. Alince, B., and van de Ven, T. G. M., *Colloids Surf. A*. **71,** 105 (1993).
3. Chen, K. M., Jiang, X. P., Kimerling, L. C., and Hammond, P. T., *Langmuir* **16,** 7825 (2000).
4. Chase, H. A., *Chem. Eng. Sci*. **39,** 1099 (1984).
5. Peula, J. M., Hidalgo-Alvarez, R., and de las Nieves, F. J. D., *J. Colloid Interface Sci*. **201,** 139 (1998).
6. Miksa, B., Wilczyńka, M., Cierniewski, C., Basinska, T., and Słomkowski, S., *J. Biomater. Sci. Polymer Ed*. **7,** 503 (1995).
7. Molina-Bolivar, J. A., Galisteo-Gonzalez, F., and Hidalgo-Alvarez, R., *Langmuir* **17,** 2514 (2001).
8. Hull, M., and Kitchener, J. A., *Trans. Faraday Soc*. **65,** 3093 (1969).
9. Serizawa, T., Kamimura, S., and Akashi, M., *Colloids Surf. A* **164,** 237 (2000).
10. Adamczyk, Z., Zembala, M., Siwek, B., and Czarnecki, J., *J. Colloid Interface Sci*. **110,** 188 (1986).
11. Adamczyk, Z., Zembala, M., Siwek, B., and Warszyński P., *J. Colloid Interface Sci*. **140,** 123 (1990).
12. Adamczyk, Z., Siwek, B., Zembala, M., and Belouschek, P., *Adv. Colloid Interface Sci*. **48,** 151 (1994).
13. Jin, X., Wang, N. H. L., Tarjus, G., and Talbot, J., *J. Phys. Chem*. **97,** 4256 (1993).
14. Jin, X., Talbot, J, and Wang, N. H. L., *AIChE J*. **40,** 1685 (1994).
15. Hinrichsen, E. L., Feder, J., and Jossang, T., *J. Stat. Phys*. **44,** 793 (1986).
16. Schaaf, P., and Talbot, J., *J. Chem. Phys*. **91,** 4401 (1989).
17. Senger, B., Voegel, J. C., and Schaaf, P., *Colloids Surf. A* **165,** 255 (2000).
18. Adamczyk, Z., Weroński, P., and Musiał, E., *J. Chem. Phys*., in press.
19. Adamczyk, Z., and Weroński, P., *J. Chem. Phys*. **108,** 9851 (1998).
20. Senger, B., Schaaf, P., Voegel, J. C., Johner, A., Schmitt, A., and Talbot, J., *J. Chem. Phys*. **97,** 3813 (1992).
21. Wojtaszczyk, P., Bonet Avalos, J., and Rubi, J. M., *Europhys. Lett*. **40,** 299 (1997).
22. Adamczyk, Z., Senger, B., Voegel, J. C., and Schaaf, P., *J. Chem. Phys*. **110,** 3118 (1999).
23. Faraudo, J., and Bafaluy, J., *J. Chem. Phys*. **112,** 2003 (2000).
24. Adamczyk, Z., *J. Colloid Interface Sci*. **229,** 477 (2000).
25. Reiss, H., Frisch, H. L., and Lebowitz, J. L., *J. Chem. Phys*. **31,** 369 (1959).
26. Adamczyk, Z., Siwek, B., and Musiał, E., *Langmuir* **17,** 4529 (2001).
27. Adamczyk, Z., Siwek, B., Zembala, M., and Weroński, P., *J. Colloid Interface Sci*. **185,** 236 (1997).
28. Adamczyk, Z., and Weroński, P., *Adv. Colloid Interface Sci*. **83,** 137 (1999).